

The substituent effect on the luminescent properties of a set of 4-amino-4H-1,2,4-triazole: Syntheses, crystal structures and Hirshfeld analyses



Yu-Rong Xi^b, Xu-Kai Chen^b, Yong-Tao Wang^b, Gui-Mei Tang^{a,*}, Xiao-Min Chen^b, Yu-Song Wu^b, Shi-Ning Wang^a

^a School of Pharmaceutical Sciences, Qilu University of Technology (Shandong Academy of Sciences), Jinan, 250353, China

^b School of Chemistry and Chemical Engineering, Qilu University of Technology (Shandong Academy of Sciences), Jinan, 250353, China

ARTICLE INFO

Article history:

Received 1 April 2021

Revised 8 June 2021

Accepted 9 June 2021

Available online 14 June 2021

Keywords:

4-amino-4H-1,2,4-triazole

Substituent effect

Crystal structures

Hydrogen bond

Packing interaction

Supramolecular interactions

Hirshfeld surface analyses

ABSTRACT

A set of compounds based on 4-amino-4H-1,2,4-triazole group, namely, 4,4'-(4-amino-4H-1,2,4-triazole-3,5-diyl)dibenzoic acid (**1**), 4,4'-(4-amino-4H-1,2,4-triazole-3,5-diyl)dianiline (**2**), 4,4'-(4-amino-4H-1,2,4-triazole-3,5-diyl)diphenol (**3**), were obtained through reacting different aromatic nitrile and hydrazine under the solvothermal conditions, respectively. The title compounds **1–3** have been characterized by IR, UV–Vis, ¹H NMR, ¹³C NMR, element analysis (EA), single crystal X-ray diffraction, and powder X-ray diffraction (PXRD). In these compounds, a plenty of hydrogen bonds (C/N–H···O/N) and C–H···π can be obviously obtained, through which a three-dimensional framework will be constructed. The solid-state luminescent spectra of **1–3** show that the emission maxima are observed at 398, 464 and 402 nm, respectively. The order of maximal peaks is **1**<**3**<**2**. The Hirshfeld surface analyses confirm that the order of the contribution of C···H/H···C and H···H contacts is **1**<**3**<**2**, which is in a good accordance with that of the luminescent bands.

© 2021 Elsevier B.V. All rights reserved.

1. Introduction

The 1,2,4-triazole is a kind of important five-membered heterocyclic compounds and has attracted considerable interest in the fields of materials, coordination chemistry and medicine due to their important biologically activities and strong coordination abilities [1–16]. Typically, the derivatives based on 1,2,4-triazole are extensively investigated as ligands [17–19] for the design and development of novel metal coordination complexes, which exhibit very interesting physical properties such as magnetism, gas absorption and optics [20–22]. Recent studies show that a Ir(III)-based complex consisting of a kind of 1,2,4-triazole displays a sky-blue emission with high quantum yields, which becomes a type of potential materials for organic light emitting diodes (OLEDs) [23]. This heterocyclic compounds have been applied to the field of material science [24], which plays an important role in energy materials [25]. Additionally, compounds with 1,2,4-triazole nuclei have been proved for a broad-spectrum activities such as fungicidal [26], herbicidal [27], anticonvulsant [28] and plant growth regulatory activities [29]. However, the design and development

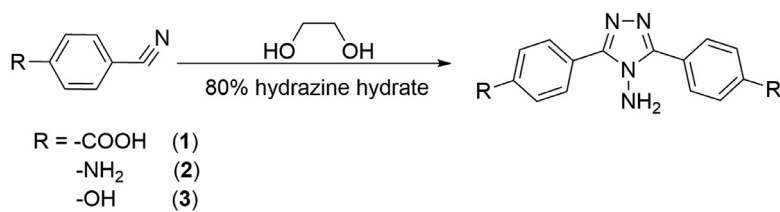
of luminescent materials with 1,2,4-triazole moieties still remains sparse. Especially, it is necessary to investigate the 4-amino-1,2,4-triazole based compounds with the controllable photoluminescent behaviours through the substituents.

Due to 1,2,4-triazoles having the promising functions, different synthetic approaches have been documented for the preparation of substituted 1,2,4-triazoles [14,30,31]. The 1,2,4-triazoles is the reaction of an appropriate aliphatic, aromatic, or heterocyclic primary amine with diformhydrazide. Despite a positive progress of the preparation for this heterocyclic compounds has been made [12], many currently available methods suffer from various limitations, including the use of hazardous and costly materials or the requirement for harsh reaction conditions [32]. Therefore, the development of more efficient, convenient and eco-friendly methods is still desired. On the other hand, solvothermal/hydrothermal methods have been extensively applied to the field of the coordination chemistry and materials chemistry [33–39], which is a simple and available route for the synthesis and preparation of metal coordination complexes and inorganic materials [40–44]. So far, the development and investigation of this method remains rare in the areas of organic chemistry.

Based on these minds mentioned above, herein, we would like to report an efficient and convenient process for the synthesis

* Corresponding authors.

E-mail address: tgm@qlu.edu.cn (G.-M. Tang).

**Scheme 1.** the preparation procedure of compounds **1–3**.

of a set of compounds based on 4-amino-4*H*-1,2,4-triazole group, namely, 4,4'-(4-amino-4*H*-1,2,4-triazole-3,5-diyl)dibenzonic acid (**1**), 4,4'-(4-amino-4*H*-1,2,4-triazole-3,5-diyl)dianiline (**2**), and 4,4'-(4-amino-4*H*-1,2,4-triazole-3,5-diyl)diphenol (**3**), were obtained through reacting different aromatic nitrile and hydrazine under the solvothermal conditions, respectively (**Scheme 1**). The spectra of FT-IR, UV-Vis, ¹H NMR and ¹³C NMR for **1–3** were studied. Additionally, the crystal structures of **1–3** have been discussed, and its fluorescence properties and thermal behaviors were investigated in details. As we expected, the substituted groups can affect the luminescent properties of these compounds with amino-triazole functions, which can be further confirmed by the Hirshfeld surface analyses.

2. Experimental

2.1. Materials and measurements

Reagents and solvents were commercially available and not further purified. C, H and N microanalyses were carried out with a Perkin-Elmer 240 elemental analyzer. Thermogravimetric analysis (TGA) data were collected with a TA SDT Q600 analyzer in N₂ at a heating rate of 10 °C min⁻¹ in the range of 10–600 °C. The FT-IR spectra were recorded from KBr pellets in the range 400–4000 cm⁻¹ on a Bruker Tensor4 spectrometer. UV-Vis absorption spectra were recorded on a SHIMADZU UV-2600 spectrophotometer with 0.1 nm resolution. The solution/solid-state fluorescence spectra were recorded on a HITACHI-4500 spectrometer at room temperature.

2.2. The synthesis of compound **1** (4CA)

To a mixture solution of ethylene glycol (10 mL) and 85% hydrazine hydrate (3.8 mL, 60 mmol), 4-cyanobenzoic acid (1.470 g, 10 mmol) were heated at 130 °C for 3 days in a 15 ml Teflon-lined vessel container. The reaction mixture was cooled to room temperature at a rate of 5 °C h⁻¹. After cooling to room temperature, pure water (30 mL) was poured to the mixture solution and it was added adjusted to pH 3 by the concentrated HCl solution. Subsequently, the mixture was cooled to room temperature. Finally, the earthy yellow crystals were collected by vacuum filtration. Yield (62.5%, 1.013 g). M.p. >300 °C. Elemental analysis calcd (%) for C₁₆H₁₂N₄O₄ (324.30): C, 59.26; H, 3.73; N, 17.28; found: C, 59.42; H, 3.72; N, 17.33. ¹H NMR (400 MHz, DMSO-*d*₆) δ: 13.10 (s, 2H), 8.19 (d, *J* = 8 Hz, 4H), 8.09 (d, *J* = 8 Hz, 4H), 6.41 (s, 2H). ¹³C NMR (100 MHz, DMSO-*d*₆) δ: 166.83, 153.86, 131.57, 130.94, 129.32, 128.37. IR (KBr, cm⁻¹): 3362(m), 3277(w), 3211(w), 2366(w), 1946(w), 1628(m), 1570(m), 1541(m), 1392(m), 1290(m), 1188(m), 1113(m), 1018(m), 966(m), 912(w), 866(m), 783(m), 717(s), 536(m).

2.3. The synthesis of **2** (4NH2)

The synthesis procedure of compound **2** was similar to that of compound **1** when the 4-aminobenzonitrile took place of 4-

cyanobenzoic acid. Yield: 0.686 g, 48.3%. M.p. 212–215 °C. Elemental analysis calcd (%) for C₁₄H₁₆N₆O (284.33): C, 63.14; H, 5.30; N, 31.56; Found: C, 63.28; H, 5.31; N, 31.50. ¹H NMR (400 MHz, DMSO-*d*₆) δ 7.67 (d, *J* = 8.2 Hz, 4H), 6.65 (d, *J* = 8.2 Hz, 4H), 5.95 (s, 2H), 5.44 (s, 4H). ¹³C NMR (101 MHz, DMSO-*d*₆) δ 154.40, 150.26, 129.56, 115.12, 113.65. IR (KBr, cm⁻¹): 3386(s), 3327(m), 3273(m), 3157(m), 2428(w), 2148(w), 2029(w), 1959(m), 1909(w), 1730(w), 1647(w), 1614(s), 1496(s), 1477(s), 1423(w), 1385(s), 1275(m), 1115(s), 1014(m), 908(w), 837(m), 810(m), 739(w), 694(m), 617(s), 571(m), 532(w), 471(w), 428(w).

2.3. The synthesis of compound **3** (4OH)

The preparation of compound **3** was similar to that of compound **1** when 4-hydroxybenzonitrile took place of 4-cyanobenzoic acid. Yield: 0.958 g, 71.4%. M.p. 290–292 °C. Elemental analysis calcd (%) for C₁₄H₁₂N₄O₂ (268.28): C, 62.68; H, 4.51; N, 20.88; Found: C, 62.79; H, 4.50; N, 20.82. ¹H NMR (400 MHz, DMSO-*d*₆) δ 9.88 (s, 2H), 7.84 (d, *J* = 8.5 Hz, 4H), 6.90 (d, *J* = 8.5 Hz, 4H), 6.69 (s, 2H). ¹³C NMR (101 MHz, DMSO-*d*₆) δ 159.02, 154.30, 130.48, 130.20, 118.67, 115.94, 115.67. IR (KBr, cm⁻¹): 3476(br), 3416(w), 3223(w), 2809(w), 2678(w), 2509(w), 2362(w), 1915(w), 1772(m), 1613(s), 1481(s), 1363(w), 1236(s), 1173(s), 1108(s), 979(m), 902(w), 842(s), 744(w), 671(w), 598(m), 534(s), 453(w).

2.4. Single-crystal structure determination

Single-crystal structures of compounds **1–3** were measured by a Bruker Smart CCD equipped with graphite-monochromator Mo K α radiation ($\lambda = 0.71073 \text{ \AA}$). The lattice parameters were obtained by a least-squares refinement of the diffraction data. All the measured independent reflections were used in the structural analysis, and semi-empirical absorption corrections were applied using the SADBASE program [45]. The program SAINT was used for integration of the diffraction profiles [46]. The structure was solved by direct methods using the SHELXS and OLEX2 program of the SHELXTL package and refined with SHELXL [47–49]. All non-hydrogen atoms were located in successive difference Fourier syntheses. The final refinement was performed by full-matrix least-squares methods with anisotropic thermal parameters for all the non-hydrogen atoms based on R^2 . The hydrogen atoms were placed in the calculated sites and included in the final refinement in the riding model approximation with displacement parameters derived from the parent atoms to which they were bonded. Special computations for the crystal structure discussions were carried out with PLATON for Windows [50]. A summary of the crystallographic data and structure refinements are listed in **Table 1**. Selected bond lengths and bond angles are summarized in Tables 2. Corresponding hydrogen bond and packing interactions data for compounds **1–3** are listed in **Tables 3** and **4**, respectively.

2.5. Hirshfeld surface analyses

The Hirshfeld surface analyses were calculated by the program of CrystalExplorer [51].

Table 1
Crystal data and structure refinement parameters for compounds **1–3**.

Compound reference	1	2	3
Chemical formula	C ₁₆ H ₁₂ N ₄ O ₄	C ₁₄ H ₁₆ N ₆ O	C ₁₄ H ₁₂ N ₄ O ₂
Formula Mass	324.30	284.33	268.28
Crystal System	Orthorhombic	Orthorhombic	Monoclinic
<i>a</i> /Å	3.7674(9)	10.9651(5)	9.4502(17)
<i>b</i> /Å	11.271(3)	16.5655(9)	7.5947(15)
<i>c</i> /Å	33.244(9)	7.1492(4)	18.190(4)
$\alpha/^\circ$	90.00	90	90
$\beta/^\circ$	90.00	90	102.089(6)
$\gamma/^\circ$	90.00	90	90
Unit cell volume/Å ³	1411.7(6)	1298.60(12)	1276.6(4)
Temperature/K	296(2)	100.00(10)	100(2)
Space group	<i>Pbcm</i>	<i>Pna2</i> ₁	<i>P2</i> ₁ / <i>n</i>
No. of formula units per unit cell, <i>Z</i>	4	4	4
Radiation type	Mo K α	Mo K α	Mo K α
Absorption coefficient, μ/mm^{-1}	0.113	0.099	0.098
No. of reflections measured	7346	5826	10,616
No. of independent reflections	1271	2807	2960
<i>R</i> _{int}	0.0601	0.1632	0.0618
Final <i>R</i> _f values ($I > 2\sigma(I)$)	0.0418	0.0379	0.0525
Final <i>wR</i> (F^2) values ($I > 2\sigma(I)$)	0.0994	0.0889	0.1388
Final <i>R</i> _f values (all data)	0.0811	0.0573	0.0646
Final <i>wR</i> (F^2) values (all data)	0.1207	0.1043	0.1467
Goodness of fit on F^2	1.015	1.116	1.056
CCDC number	1,422,655	2,067,982	2,067,983

^a $R_1 = \sum |F_o| - |F_c| / \sum |F_o|$. ^b $wR_2 = [\sum [w(F_o^2 - F_c^2)^2] / \sum [w(F_o^2)]^{1/2}]^{1/2}$.

3. Results and discussion

3.1. Description of the crystal structures

3.1.1. Structure of **1** (**4CA**)

Single X-ray analysis for the compound **4CA** reveals that it crystallizes in the form of centrosymmetric space group *Pbcm* with the orthorhombic system. There exists half molecule of **44CA** in a symmetric unit (Fig. 1a). The dihedral angle between the central triazole ring and the phenyl ring is 40.6°, being obviously higher than those found in other amino-triazole-based compounds. The bond distances of N–N, C–N and C = N range from 1.316(3) to 1.417(4) Å, being similar to those in other compounds with amino-triazole functional group. It is worthy to mention that the free ligand **4CA** does not form molecular zwitterions, which is different from that found in 2-(1*H*-benzotriazol-1-yl) acetic acid [52–53]. Each **4CA** molecule making use of the carboxylate group in the formation of head-tail forms a type of intermolecular hydrogen bonds (O(1)–H(1)•••O(2)^a, 1.83 Å, ^a-x,1-y,1-z) (Table 2). Through the hydrogen bond interactions, **4CA** molecules are linked into a 1-D wave-like chain along the crystallographic *c* axis (Fig. 1b). Additionally, the triazole groups of two **4CA** molecules form another kind of intermolecular hydrogen bonds (N(3)–H(3B)•••N(2)^b, 2.15 Å, ^b1-x,1/2+y,3/2-z; N(3)–H(3B)•••N(2)^c, 2.53 Å, ^c-1+x,y,z) (Table 2). These hydrogen bonds lie parallel to each other resulting in a two-dimensional (2D) supramolecular layer along the *bc* plane. It is interestingly observed in the 2D array, there are two types of hydrogen-bonded patterns A–D, noted as $R_2^2(8)$ (Fig. 5c(A)) and $R_6^3(40)$ (Fig. 5c(B)), respectively. These 2D layers are further extended into a three-dimensional (3D) supramolecular framework through two kinds of offset π ••• π packing interactions between aromatic rings. One originates from two triazole groups (3.7674(18) Å) and another does from two phenyl groups (3.7675(17) Å) (Fig. 1d).

3.1.2. Structure of **2** (**4NH2**)

When 4-amino phenyl nitrile replaced the 4-cyanobenzoic acid, a new compound **2** can be obtained under the similar reaction conditions. Single-crystal X-ray diffraction analysis reveals that compound **2** belongs to the orthorhombic system with the *Pna2*₁

space group. The asymmetric unit contains one **4NH2** molecule and one free water molecule (Fig. 2a). The bond distances among the triazole ring fall in the range of 1.308(6)–1.453(10) Å, which can be found in other amino-triazole compounds. Two dihedral angles between the phenyl rings and the triazole ring are 37.3 and 35.2°, being obviously smaller than that of compound **1**.

In supramolecular structures, hydrogen bonds and stacking interactions can often be observed. As shown in Fig. 2 and Table 3, three types of hydrogen bonds were observed in compound **1**, such as: (a) The N–H•••N (N1–H1A•••N2^a 3.114(3) Å, ^a-1/2+x,1/2-y,z; N5–H5A•••N6^b 3.197(4) Å, ^b1/2-x,-1/2+y,-1/2+z; N5–H5B•••N1^c 3.406(4) Å, ^c1/2-x,1/2+y,-1/2+z; N6–H6B•••N3^d 3.047(3) Å, ^d-1/2+x,3/2-y,z) intermolecular hydrogen bonds occur among different nitrogen atoms of different **4NH2** molecules. (b) The N–H•••O (N1–H1B•••O1^b 3.024(3) Å, ^b1/2-x,-1/2+y,-1/2+z; O1–H1D•••N1^a 3.065(3) Å, ^a-1/2+x,1/2-y,z; N6–H6A•••O1^c 3.158(3) Å, ^c1/2-x,1/2+y,-1/2+z) intermolecular hydrogen bonds originate from the nitrogen atoms of the **4NH2** molecule and the oxygen atoms of the crystallized water molecules. (c) The hydrogen bond of O1–H1D•••N1^a (^a-1/2+x,1/2-y,z) with the distance of 3.065(3) Å can be found between the oxygen atom of water molecular and the nitrogen atom of phenylamino group of **4NH2**. Except from these hydrogen bonds, the π ••• π and C–H••• π packing interactions can be found in compound **2**. For example, there exist the interactions such as Cg1•••Cg1^a(^a1-x,1-y,-1/2+z), Cg1•••Cg1^b(^b1-x,1-y,1/2+z), C2–H2•••Cg3^c(^c1/2-x,-1/2+y,1/2+z), C5–H5•••Cg3^d(^d1-x,1-y,-1/2+z), C11–H11•••Cg2^e(^e1/2-x,1/2+y,1/2+z) as well as C14–H14•••Cg2^a with the distances of 3.6405(18), 3.6404(18), 3.388(3), 3.343(3), 3.345(3) and 3.515(3) Å, respectively. The Cg1 and Cg2 and Cg3 represent the centers of N2–N3–C8–N4–C7, C1–C2–C3–C4–C5–C6 and C9–C10–C11–C12–C13–C14, respectively.

In Fig. 2b, through the N1–H1B•••O1^b intermolecular hydrogen bonds, the crystallized water molecules and the **4NH2** molecules alternatively link to supramolecular congregation. Further, through the hydrogen bonds of N6–H6A•••O1^c, the adjacent congregation can be expanded to a supramolecular 1D chain along the crystallographic *b* direction. Then, the hydrogen bonds of N1–H1A•••N2^a and N6–H6B•••N3^d make the adjacent 1D chains ex-

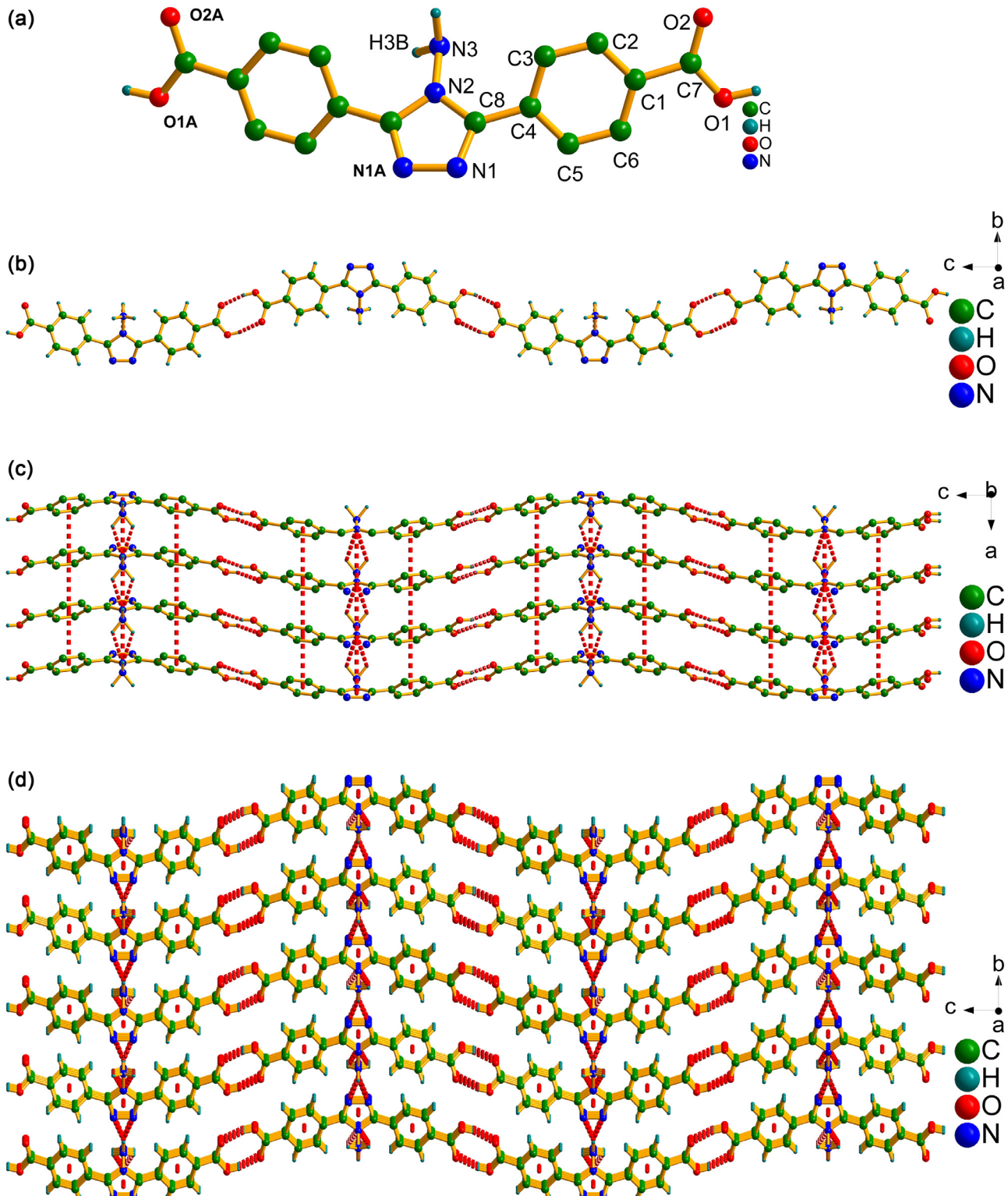


Fig. 1. (a) A perspective view of **1**. (b) The 1D chain through hydrogen bonds along the *c* axis. (c) The 2D supramolecular network formed by hydrogen bonds in **1**. (d) The packing diagram of **1**.

Table 2
Selected bond lengths (Å) and angles (°) for complexes **1–3**.

Bond lengths/bond angles	Bond lengths (Å)/Bond angles (°)	Bond lengths/bond angles	Bond lengths (Å)/Bond angles (°)
1			
O1-C7	1.289(3)	O2-C7	1.243(3)
N1-C8	1.316(3)	N1-N1 ^a	1.392(3)
N2-N3	1.417(4)	N2-C8	1.368(3)
N2-C8 ^a	1.368(3)	C1-C2	1.392(3)
C1-C6	1.387(3)	C1-C7	1.487(3)
C2-C3	1.378(3)	C3-C4	1.395(3)
C4-C5	1.393(3)	C4-C8	1.468(3)
C5-C6	1.380(3)		
C8-N1-N1 ^a	107.54(19)	N3-N2-C8	126.25(13)
N3-N2-C8 ^a	126.25(13)	C8-N2-C8 ^a	106.0(2)
C2-C1-C6	119.6(2)	C2-C1-C7	119.0(2)
C6-C1-C7	121.4(2)	C1-C2-C3	120.7(2)
C2-C3-C4	119.7(2)	C3-C4-C5	119.5(2)
C3-C4-C8	121.5(2)	C5-C4-C8	119.0(2)
C4-C5-C6	120.5(2)	C1-C6-C5	120.0(2)
O1-C7-O2	123.9(2)	O1-C7-C1	115.7(2)
O2-C7-C1	120.4(2)	N1-C8-N2	109.4(2)
N1-C8-C4	125.3(2)	N2-C8-C4	125.3(2)
2			
N1-C1	1.402(3)	N2-N3	1.385(3)
N2-C7	1.319(3)	N3-C8	1.312(3)
N4-N5	1.433(3)	N4-C7	1.367(3)
N4-C8	1.364(3)	N6-C12	1.394(3)
C1-C2	1.395(3)	C1-C6	1.403(3)
C2-C3	1.381(4)	C3-C4	1.398(3)
C4-C5	1.395(4)	C4-C7	1.467(4)
C5-C6	1.380(4)	C8-C9	1.469(3)
C9-C10	1.397(3)	C9-C14	1.400(3)
C10-C11	1.381(4)	C11-C12	1.400(4)
C12-C13	1.398(3)	C13-C14	1.376(4)
N3-N2-C7	107.8(2)	N2-N3-C8	107.7(2)
N5-N4-C7	126.7(2)	N5-N4-C8	126.5(2)
C7-N4-C8	106.3(2)	N1-C1-C2	120.4(2)
N1-C1-C6	121.0(2)	C2-C1-C6	118.6(2)
C1-C2-C3	120.7(2)	C2-C3-C4	120.8(2)
C5-C4-C7	119.5(2)	C4-C5-C6	121.0(2)
C1-C6-C5	120.5(2)	N2-C7-N4	108.9(2)
N2-C7-C4	125.2(2)	N4-C7-C4	125.8(2)
N3-C8-N4	109.4(2)	N3-C8-C9	124.5(2)
N4-C8-C9	126.1(2)	C8-C9-C10	123.1(2)
C8-C9-C14	118.2(2)	C10-C9-C14	118.4(2)
C9-C10-C11	120.4(2)	C10-C11-C12	121.2(2)
N6-C12-C11	121.0(2)	N6-C12-C13	120.8(2)
C11-C12-C13	118.1(2)	C12-C13-C14	120.8(2)
C9-C14-C13	121.1(2)		
3			
O1-C1	1.354(2)	O2-C12	1.358(2)
N1-N2	1.3884(19)	N1-C7	1.311(2)
N2-C8	1.316(2)	N3-N4	1.408(2)
N3-C7	1.370(2)	N3-C8	1.363(2)
C1-C2	1.393(2)	C1-C6	1.391(2)
C2-C3	1.380(2)	C3-C4	1.392(2)
C4-C5	1.395(2)	C4-C7	1.462(2)
C5-C6	1.380(2)	C8-C9	1.467(2)
C9-C10	1.388(2)	C9-C14	1.394(2)
C10-C11	1.384(2)	C11-C12	1.393(2)
C12-C13	1.388(2)	C13-C14	1.379(2)
N2-N1-C7	107.99(13)	N1-N2-C8	107.56(12)
N4-N3-C7	128.64(13)	N4-N3-C8	123.93(13)
C7-N3-C8	106.55(13)	O1-C1-C2	119.06(14)
O1-C1-C6	121.08(14)	C2-C1-C6	119.86(15)
C1-C2-C3	119.52(15)	C2-C3-C4	121.12(15)
C3-C4-C5	118.88(15)	C3-C4-C7	119.63(14)
C5-C4-C7	121.49(14)	C4-C5-C6	120.37(15)
C1-C6-C5	120.23(15)	N1-C7-N3	108.83(14)
N1-C7-C4	126.56(14)	N3-C7-C4	124.60(14)
N2-C8-N3	109.06(14)	N2-C8-C9	125.54(14)
N3-C8-C9	125.39(14)	C8-C9-C10	119.39(14)
C8-C9-C14	121.76(14)	C10-C9-C14	118.85(15)
C9-C10-C11	121.06(15)	C10-C11-C12	119.43(14)
O2-C12-C11	117.89(14)	O2-C12-C13	122.20(15)
C11-C12-C13	119.85(15)	C12-C13-C14	120.13(15)
C9-C14-C13	120.54(15)		

Symmetry codes: *axe,y,3/2-z* for **1**.

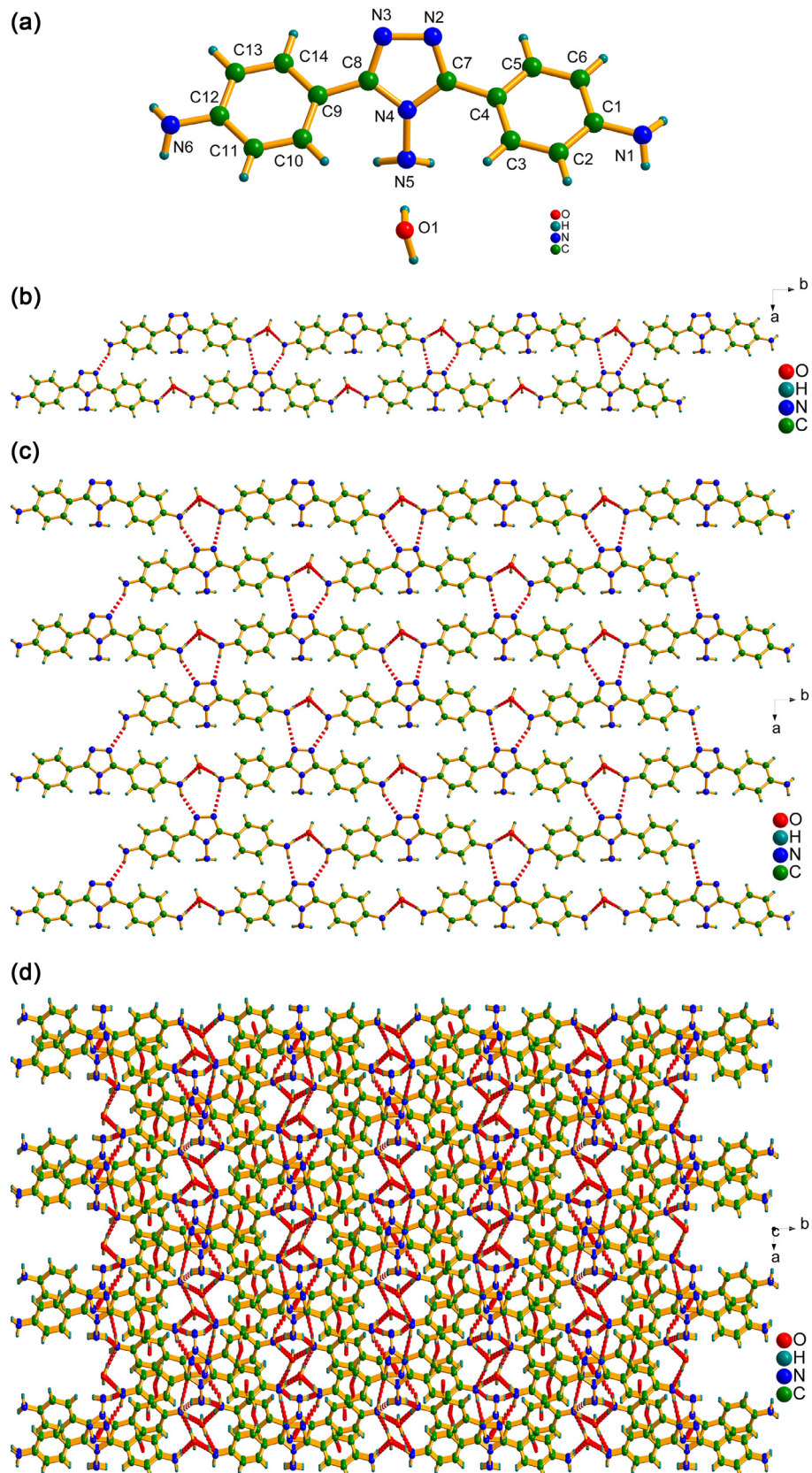


Fig. 2. (a) A perspective view of **2**. (b) The 1D supramolecular chain along the crystallographic *b* direction. (c) The 2D supramolecular network formed by hydrogen bonds along the crystallographic *ab* plane in **2**. (c) The packing diagram of **2** along the crystallographic *a* axis.

Table 3Hydrogen bond geometries in the crystal structure of compounds **1–3**, respectively.

Compounds	D-H \cdots A ^a	H \cdots A (Å)	D \cdots A (Å)	D-H \cdots A (°)
1	O1-H1 \cdots O2 ^a	1.83	2.643(3)	159
	N3-H3A \cdots N1 ^b	2.15	3.176(4)	161
	N3-H3B \cdots N2 ^c	2.53	3.288(4)	122
2	N1-H1A \cdots N2 ^a	2.26	3.114(3)	176
	N1-H1B \cdots O1 ^b	2.06(4)	3.024(3)	174(3)
	O1-H1D \cdots N1 ^a	2.17(4)	3.065(3)	167(4)
	N5-H5A \cdots N6 ^b	2.33(4)	3.197(4)	159(3)
	N5-H5B \cdots N1 ^c	2.60(4)	3.406(4)	143(3)
	N6-H6A \cdots O1 ^c	2.30	3.158(3)	172
	N6-H6B \cdots N3 ^d	2.25	3.047(3)	153
3	O1-H1 \cdots N1 ^a	2.61	3.314(2)	142
	O1-H1 \cdots N2 ^a	2.00	2.8362(19)	173'
	O2-H2 \cdots N1 ^b	2.00	2.806(2)	162
	N4-H4A \cdots O1 ^c	2.41	3.282(2)	170
	N4-H4B \cdots O2 ^d	2.50	3.275(2)	146

Symmetry codes:

^a-x,1-y,1-z.^b1-x,1/2+y,3/2-z.^c-1+x,y,z for **1**. ^a-1/2+x,1/2-y,z.^b1/2-x,-1/2+y,-1/2+z.^c1/2-x,1/2+y,-1/2+z.^d-1/2+x,3/2-y,z for **2**. ^a1/2+x,1/2-y,1/2+z.^b-1+x,y,z.^c1-x,-y,z.^d-1/2-x,1/2+y,-1/2-z for **3**.**Table 4** $\pi\cdots\pi$ and C-H \cdots π geometries in the crystal structure of compounds **1–3**.

Compounds	Cg \cdots Cg	$\pi\cdots\pi$ (Å)	C-H \cdots Cg	C-H \cdots π (Å)
1	Cg1 \cdots Cg1 ^a	3.7674(18)		
	Cg1 \cdots Cg1 ^b	3.7674(18)		
	Cg1 \cdots Cg1 ^c	3.7674(18)		
	Cg1 \cdots Cg1 ^d	3.7674(18)		
	Cg2 \cdots Cg2 ^a	3.7675(17)		
	Cg2 \cdots Cg2 ^b	3.7673(17)		
2	Cg1 \cdots Cg1 ^a	3.6405(18)	C2-H2 \cdots Cg3 ^c	3.388(3)
	Cg1 \cdots Cg1 ^b	3.6404(18)	C5-H5 \cdots Cg3 ^d	3.343(3)
			C11-H11 \cdots Cg2 ^e	3.345(3)
			C14-H14 \cdots Cg2 ^a	3.515(3)
3		3.841	C10-H10 \cdots Cg2 ^a	3.3198(18)
			C14-H14 \cdots Cg3 ^b	3.5925(19)

Symmetry codes: ^a-1+x,y,z.^b1+x,y,z.^c-1+x,y,3/2-z.^d1+x,y,3/2-Z for **1**. ^a1-x,1-y,-1/2+z.^b1-x,1-y,1/2+z.^c1/2-x,-1/2+y,1/2+z.^d1-x,1-y,-1/2+z.^e1/2-x,1/2+y,1/2+z for **2**. ^a1/2-x,-1/2+y,-1/2-z.

^b-1/2-x,1/2+y,-1/2-z for **3**. Cg1 = N1-C8-N2-C8^a-N1^a; Cg2 = C1-C2-C3-C4-C5-C6 for **1**. Cg1 = N2-N3-C8-N4; Cg2 = C7 C1-C2-C3-C4-C5-C6; Cg3 = C9-C10-C11-C12-C13-C14 for **2**. Cg2 = C1-C2-C3-C4-C5-C6; Cg3 = C9-C10-C11-C12-C13-C14 for **3**.

tend to a supramolecular 2D sheet along the crystallographic *ab* plane (Fig. 2c). Finally, there exist the $\pi\cdots\pi$ and C-H \cdots π packing interactions (Cg1 \cdots Cg1^a, Cg1 \cdots Cg1^b, C2-H2 \cdots Cg3^c, C5-H5 \cdots Cg3^d and C11-H11 \cdots Cg2^e) and hydrogen bonds such as N5-H5A \cdots N6^b, N5-H5B \cdots N1^c as well as O1-H1D \cdots N1^a. Based on these supramolecular interactions, a supramolecular 3D architecture can be generated along the crystallographic *c* direction (Fig. 2d).

3.3. Structure of **3** (**4OH**)

When 4-hydroxyl phenyl nitrile took place of 4-cyanobenzoic acid, a new compound **3** can be obtained under the similar reaction conditions. The results of X-ray crystal diffraction analysis show that compound **3** belongs to the space group of $P2_1/n$ with

the monoclinic system, being different from the reported compound in the literature [54]. The asymmetric unit is comprised of one **4OH** molecule (Fig. 3a). The bond lengths among the triazole ring range from 1.311(2) to 1.3884(19) Å, which can be observed in literature. Two dihedral angles with 38.5 and 41.6° can be observed between the phenyl rings and the triazole ring, which are comparable to that found in compound **1** and obviously larger than that observed in compound **2**.

It often happen the hydrogen bonds and C-H \cdots π stacking interactions in the supramolecular structures. In compound **3**, it occurs N-H \cdots O intermolecular hydrogen bonds: (a) The N4-H4A \cdots O1^c (^c1-x,-y,-z) and N4-H4B \cdots O2^d (^d-1/2-x,1/2+y,-1/2-z) hydrogen bond comes from the amino-nitrogen atoms of triazole ring and the hydroxyl oxygen atoms, where the bond distance are 3.282(2) and 3.275(2) Å, respectively. (b) The hydrogen bonds of O-H \cdots N can be observed among the hydroxyl oxygen atoms and the triazole-yl nitrogen atoms. For instances, it occur the hydrogen bonds of O1-H1 \cdots N1^a (^a1/2+x,1/2-y,1/2+z), O1-H1 \cdots N2^a and O2-H2 \cdots N1^b (^b-1+x,y,z), where the bond lengths are 3.314(2), 2.8362(19) and 2.806(2) Å, respectively. Apart from these hydrogen bonds, we can find the C-H \cdots π packing interactions such as C10-H10 \cdots Cg2^a (^a1/2-x,-1/2+y,-1/2-z) and C14-H14 \cdots Cg3^b (^b-1/2-x,1/2+y,-1/2-z), where the bond distances are 3.3198(18) and 3.5925(19) Å, respectively. The rings of Cg2 and Cg3 indicate two phenyl centers.

As shown in Fig. 3b, a supramolecular 1D chain can be formed along the crystallographic *a* direction through the hydrogen bonds of O2-H2 \cdots N1^b. Through the hydrogen bonds of N4-H4B \cdots O2^d and C-H \cdots π stacking interactions of C10-H10 \cdots Cg2^a and C14-H14 \cdots Cg3^b, the adjacent supramolecular 1D chains can be expanded to a supramolecular 2D sheet along the crystallographic *ab* plane (Fig. 2c). Then, the O1-H1 \cdots N1^a, O1-H1 \cdots N2^a and N4-H4A \cdots O1^c hydrogen bonds make the adjacent layers form a supramolecular 3D framework along the crystallographic *a* direction (Fig. 3d). Notably, the shortest stacking distances (3.841 Å) can be observed between two phenyl rings.

The superposition of the moieties containing bis-phenyl amino-triazole group in compounds **1–3** is shown in Fig. S1. As shown in Fig. S1, in compounds **1** and **3**, all atoms are not located in the same plane, revealing that it does happen the obvious dihedral angles between the triazole group and phenyl ring. However, there does exist a small dihedral angle between the same aromatic rings in compound **2**. The present results may be responsible for the luminescent properties mentioned below.

3.3. IR spectra

The IR spectra of compounds **1–3** containing amine-triazole moieties are shown in Fig. S2. As shown in Fig. S2, the characteristic bands of the carboxylate group in the usual region at 1628 cm⁻¹ for the asymmetric stretching and at 1392 cm⁻¹ for the symmetric stretching. The moderate peak at 1290 cm⁻¹ suggests the presence of v_{C-O} stretching vibration of the **1**. The peak of 937 cm⁻¹ is attributed to δ_{O-H} bending vibration. The bands are located at 1650 cm⁻¹ and 1450 cm⁻¹ for **1**, which suggests the v_{C=N/C} stretching vibrations of the aromatic rings of **1**. The bending vibration of C-N can be observed at the range of 1392–1188. The peak located at 783 cm⁻¹ indicates the existence of the benzene ring. The band located at 3211 cm⁻¹ can be ascribed to the v_{C-H} stretching vibration of phenyl rings.

For compound **2**, the strong band located at 3386 cm⁻¹ can be ascribed to the characteristic v_{-OH} stretching vibration of the water molecule. The characteristic vibration peak of v_{NH} can be observed at 3327 cm⁻¹, suggesting that there exist the amino groups in the skeleton. The bands can be observed at the range of 1614–1477 cm⁻¹, which can be assigned to the v_{C=C/N} stretching vibra-

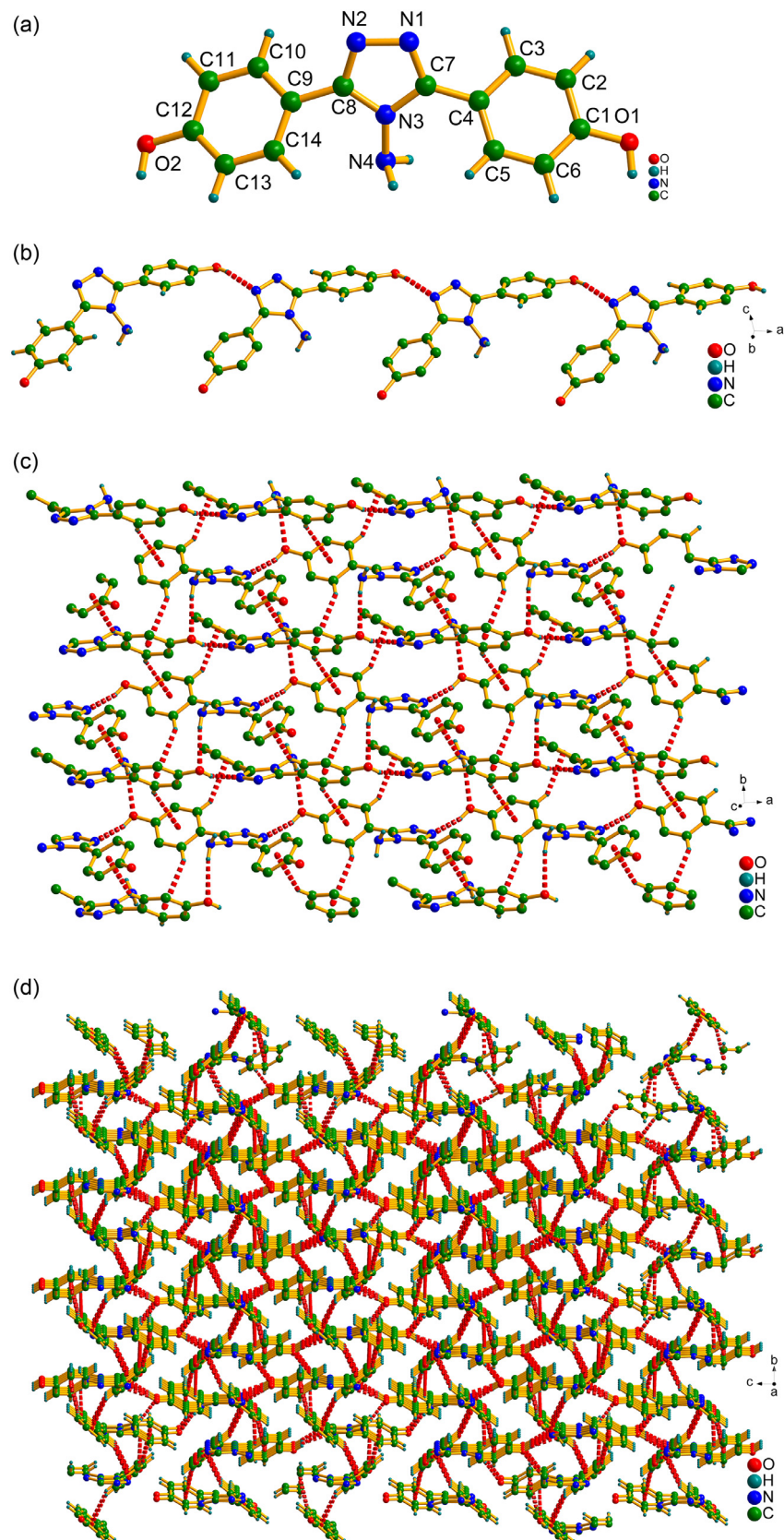
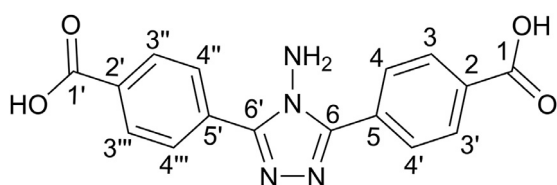


Fig. 3. (a) A perspective view of **3**. (b) The 1D chain through hydrogen bonds along the *a* axis. (c) The 2D supramolecular network formed by hydrogen bonding interactions in **3**. (d) The packing diagram of **3**.

**Scheme 2.** The structure of the 1.

tion of the phenyl and the triazole-yl rings. The bands range from 1385 to 1115 cm⁻¹, indicating the existence of the bending vibrations of aromatic C-N. The bands located at the range of 908–617 cm⁻¹ can be assigned to the in-plane and out-plane bending vibration of $\gamma_{(\text{CH})}$ and $\delta_{(\text{CH})}$ modes of aromatic rings.

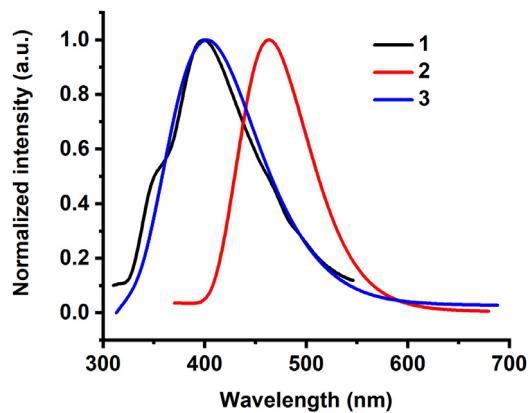
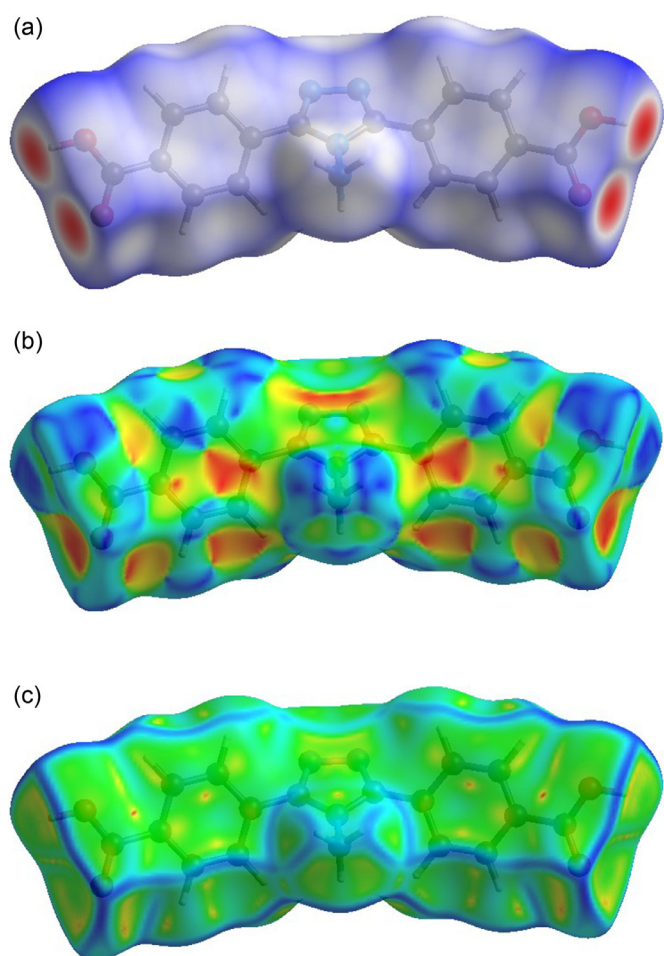
For compound **3**, we can find the broad band located at 3476 cm⁻¹, which can be attributed to the hydroxylc and amino stretching vibration. The aromatic C-H stretching vibration can be observed at 3223 cm⁻¹. The bands 1613 and 1481 cm⁻¹ can be assigned to the $\nu_{\text{C}=\text{C}}$ and $\nu_{\text{C}=\text{N}}$ stretching vibration of the aromatic rings. The bending vibrations of aromatic C-N change from 1363 to 1173 cm⁻¹. The bands can be found in the range of 979–671 cm⁻¹, indicating the existence of C-H from the phenyl groups.

3.4. UV-Vis spectra

The electronic spectral data of **1**, **2** and **3** at 2.08×10^{-5} mol L⁻¹ in dimethyl sulfoxide (DMSO) as solution have been examined (Fig. S3). The UV-vis spectra of the compounds **1–3** show that there exists one strong absorption band at 293, 295 and 295 nm, respectively. The present results may be assigned to $\pi^* \rightarrow \pi$ electronic transition of the aromatic rings [55–57].

3.5. NMR spectra

The ¹H and ¹³C NMR spectra for the target compounds were recorded in DMSO-*d*₆ as solvent and the data are given in the experimental section, which are shown in Fig. S4 and S5, respectively. The atomic labels of the title compounds are shown in **Scheme 2**. As shown in Fig. S4, there are four types of hydrogen atoms in compounds **1–3**. For compound **1**, the single peak for the carboxylic -OH group occurs at 13.10 ppm (Fig. S4a). For compounds **2** and **3**, the single signals for the -NH₂ and -OH groups bonded to the phenyl ring can be observed at 5.44 and 9.88 ppm, respectively (Fig. S4b and S4c). Two doublet signals with the coupling constant of 8 Hz at 8.20 and 8.10 ppm are assigned to aromatic protons in the ¹H NMR spectrum of **1**. The phenyl protons can be observed with the doublet signals located at 7.67 and 6.65 ppm (both coupling constant are 8.2 Hz), 7.84 and 6.90 ppm with both coupling

**Fig. 4.** Fluorescent emission spectra of compounds **1–3** in the solid state at room temperature.**Fig. 5.** Hirshfeld surface mapped with d_{norm} (a), shape index (b) and curvedness (c) of compound **1**.

constant are 8.5 Hz for compounds **2** and **3**, respectively. The protons of -NH₂ group connected to triazole ring give a single peak at 6.41, 5.95 and 6.69 ppm for compounds **1–3**, respectively.

The structures of compounds **1–3** can be further confirmed by ¹³C NMR data, which are in a good agreement with those of the ¹H NMR, IR and crystal structures (Fig. S5). The carboxylic carbons (C_1 and $C_{1'}$) occur at 166.83 ppm in compound **1**. The signal observed at 153.86, 154.40 and 159.02 ppm can be attributed to the triazole carbons (C_6 and $C_{6'}$) for compounds **1–3**, respectively. Additionally, the signals appeared at the range of 131.57–128.37, 150.26–113.65, and 154.30–115.67 ppm are assigned to phenyl carbons (C_5 , $C_{5'}$; C_2 , $C_{2'}$; C_3 , $C_{3'}$, $C_{3''}$, $C_{3'''}$ and C_4 , $C_{4'}$, $C_{4''}$, $C_{4'''}$) for compounds **1–3**, respectively. Thus, the structures for **1–3** were identified by the spectra of ¹H and ¹³C NMR, which is in a good accordance with the crystal structures mentioned above.

3.6. Powder X-ray diffraction

In order to confirm the pure phase of **1–3**, the powder X-ray diffraction (PXRD) were investigated. As illustrated in Fig. S6, the peak positions of the simulated and experimental PXRD patterns are in a good accordance with each other. The present results show that there exists a pure phase for the target products [58].

3.7. Thermogravimetric analysis

To evaluate the thermal stable properties of these compounds, the primarily thermogravimetric experiment on samples contain-

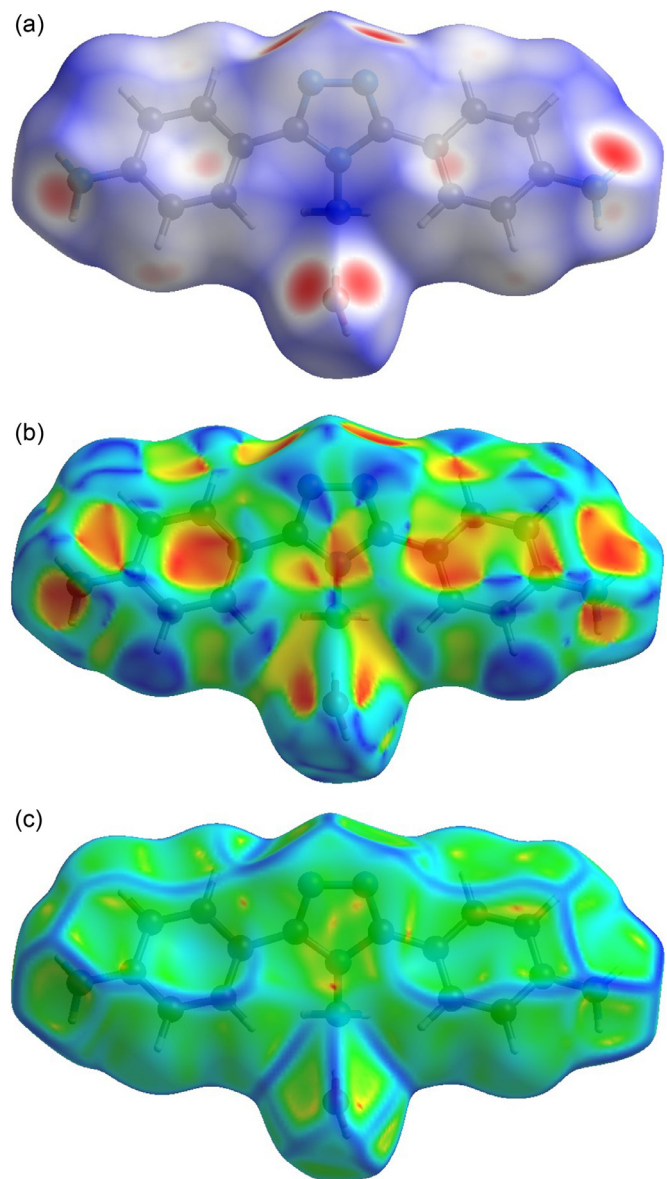


Fig. 6. Hirshfeld surface mapped with d_{norm} (a), shape index (b) and curvedness (c) of compound 2.

ing powdered crystals was taken under N_2 atmosphere with heat rate of $10\text{ }^{\circ}\text{C min}^{-1}$ [59]. The thermogravimetric analysis (TGA) results are shown in Fig. S7. The TGA curve of **1** shows that there exists a platform until $318\text{ }^{\circ}\text{C}$, indicating that compound **1** has high thermal stability. After that, it suffers a sharp weight loss up to $600\text{ }^{\circ}\text{C}$. For compound **2**, it occurs a plateau from room temperature to $110\text{ }^{\circ}\text{C}$. After that, the loss weight occurs at the range of $110\text{ }^{\circ}\text{C} - 145\text{ }^{\circ}\text{C}$, suggesting the loss of the crystallized water molecules (calcd. 6.3% and obsd. 6.3%). Then, a second platform can be observed between $145\text{ }^{\circ}\text{C}$ and $318\text{ }^{\circ}\text{C}$. Then, there exists a weight loss, being corresponded to the decomposition of the organic compound. For compound **3**, we can find a platform between the room temperature and $322\text{ }^{\circ}\text{C}$, suggesting that compound **3** has a high thermal stability. Then, the loss weight occurs, which can be assigned to the decomposition of organics.

3.8. Luminescent properties

To examine the optic properties of the title compounds, the solid-state photoluminescence of **1–3** was investigated at room

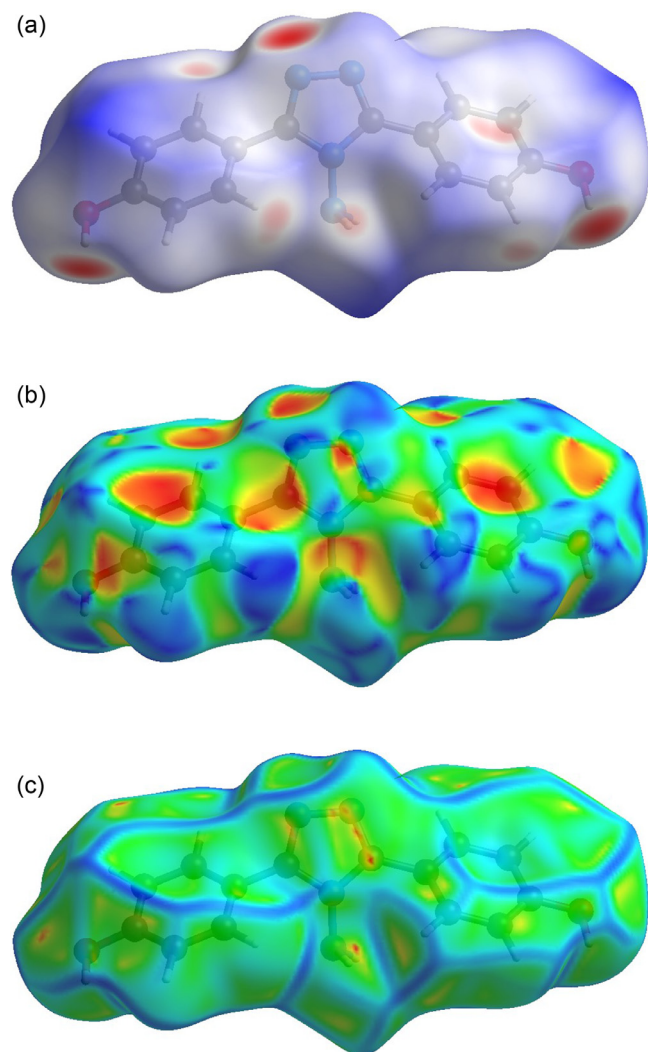


Fig. 7. Hirshfeld surface mapped with d_{norm} (a), shape index (b) and curvedness (c) of compound 3.

Table 5
Bonding contacts of compounds **1–3**.

	1	2	3
H••H (%)	32.2	41.0	33.5
H••N/N••H (%)	12.9	16.2	16.0
H••O/O••H (%)	22.8	6.5	14.3
C••H/H••C (%)	12.3	30.2	29.0

temperature [38–39]. As shown in Fig. 4, the spectra of compounds **1–3** show that the maximal emission peaks occur at 398, 464 and 402 nm with an excitation wavelength of 290, 350 and 295 nm, respectively. Notably, we can find that there exists an order of the maximal bands for these compounds as the following: **1**<**3**<**2**. Compared the maximal peak of compound **1**, those of compounds **2** and **3** show obvious red-shift phenomena. The red-shifted values are about 74 and 4 nm for compounds **2** and **3**, respectively. The observed phenomena can be ascribed to the difference of electron-acceptor/donor groups. There exists the order of electron-donor groups: $-\text{COOH} < -\text{OH} < -\text{NH}_2$, which is in a good agreement with that of the maximal peaks. The present luminescent results reveal that the optic property can be easily tuned by the substituents.

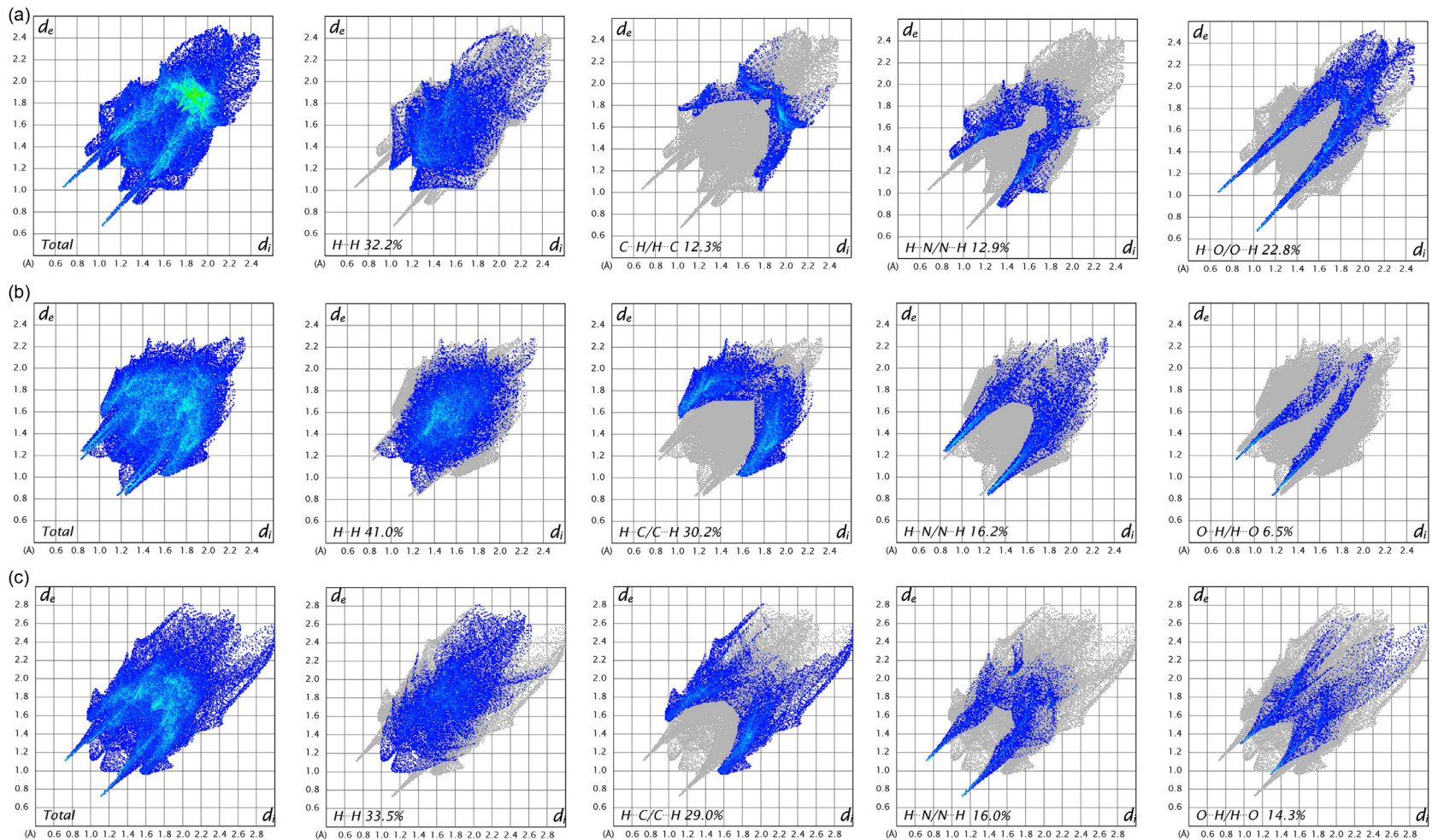


Fig. 8. Finger print plots (a, b and c) of compounds **1–3**, resepctively.

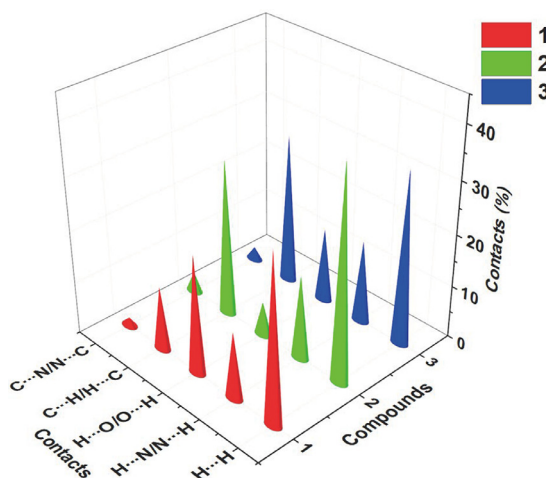


Fig. 9. Bonding contacts of compounds **1–3**.

3.9. Hirshfeld surface analyses

To evaluate the relationship between the intermolecular interactions and the luminescent properties, the Hirshfeld surface analyses were performed. The Hirshfeld surface and the corresponding two-dimension fingerprint plots visualize the intermolecular interactions. The distances d_e and d_i are on behalf of the closest atom from the Hirshfeld surface outside and inside, respectively, which can be enabled to analysis the intermolecular contacts by mapping of d_{norm} (distance equal to the Vander Waals radii). As shown in Fig. 5a, the deep red spots describe the $\text{H}\cdots\text{H}$ (32.2%) and $\text{O}\cdots\text{H}/\text{O}\cdots\text{H}$ (22.8%) bonding contacts contribution, represent the carboxylic bonding contact (Fig. 8a). Furthermore, the $\text{H}\cdots\text{N}/\text{N}\cdots\text{H}$ and $\text{C}\cdots\text{H}/\text{H}\cdots\text{C}$ weak contacts contribute 12.9% and 12.3%, respectively, which were described in blue regions in Fig. 5a. Three circles in compound **1** described in red areas in shape index represent the hollows and the bump shown in blue (Fig. 5b) [60]. As the curvedness expressed (Fig. 5c), all atoms are located in a plane. In compound **2**, the type of $\text{H}\cdots\text{H}$ (41.0%), $\text{C}\cdots\text{H}/\text{H}\cdots\text{C}$ (30.2%), $\text{N}\cdots\text{H}/\text{H}\cdots\text{N}$ (16.2%) and $\text{O}\cdots\text{H}/\text{H}\cdots\text{O}$ (6.5%) bonding contacts contribute the most interactions of total molecule (Fig. 8b) and show in the red spots (Fig. 6a). The contribution of other weak contacts is listed as the following: $\text{C}\cdots\text{N}/\text{N}\cdots\text{C}$ (3.9%), $\text{C}\cdots\text{O}/\text{O}\cdots\text{C}$ (0.0%), $\text{N}\cdots\text{N}$ (1.8%), $\text{O}\cdots\text{N}/\text{N}\cdots\text{O}$ (0.0%), $\text{O}\cdots\text{O}$ (0.0%) and $\text{C}\cdots\text{C}$ (0.2%) (Fig. S8). As shown in Fig. 7a, in compound **3**, the bright red spots in the Hirshfeld surface indicate the strong connections of $\text{H}\cdots\text{O}/\text{O}\cdots\text{H}$, $\text{N}\cdots\text{H}/\text{H}\cdots\text{N}$ and $\text{C}\cdots\text{H}/\text{H}\cdots\text{C}$, which contribute 14.3%, 16.0% and 29.0% to the whole interactions, respectively. They show two sharp spikes (Fig. 8c and Fig. 9). Notably, the $\text{H}\cdots\text{H}$ contribution can be found to be 33.5%. The bonding contacts of compounds **1–3** are collected in Table 5 and Fig. 9.

As shown in Table 5, Fig. 8 and Fig. 9, we can find that the $\text{H}\cdots\text{H}$ contribution with 32.2%, 41.0% and 33.5% can be observed for compounds **1–3**, respectively. Obviously, the order of $\text{H}\cdots\text{H}$ contribution is following: **1**<**3**<**2**. Notably, the difference of $\text{H}\cdots\text{H}$ contribution between compounds **1** and **2** is 1.3%, while that between compounds **1** and **3** is 8.8%. Obviously, the difference value in the former is significantly smaller than that in the latter. The present order and magnitude are in a good agreement with those of luminescent for these compounds. Surprisingly, there exists the same order of $\text{C}\cdots\text{H}/\text{H}\cdots\text{C}$ bonding contacts as mentioned above. The present results can be responsible for the order of the maximal bands in compounds **1–3**.

4. Conclusion

In summary, we have successfully synthesized a set of 3,5-disubstituted-4-amine-1,2,4-triazole with different functional groups through a convenient method under the solvothermal reaction conditions. The title compounds are characterized by EA, IR, NMR, UV-Vis spectra, single-crystal X-ray diffraction, and powder X-ray diffraction. The photoluminescent properties can not only be mediated through the substituents, but also the maximal peaks are proportional to the electron-donor capacities of the substituted groups. The Hirshfeld surface analyses further reveal that there exists the same order of the $\text{H}\cdots\text{H}$ and $\text{C}\cdots\text{H}/\text{H}\cdots\text{C}$ bonding contacts, which are in a good accordance with the luminescent order. The present strategy gives us a platform to develop and design the novel luminescent materials. Currently, 4-amine-1,2,4-triazole based compounds displaying the promising photoluminescent materials are explored.

Author statement

Yu-Rong Xi: Data curation, Writing-Original draft preparation.
Xu-Kai Chen: Data Curation, Investigation, Resources
Yong-Tao Wang: Supervision, Writing - Review & Editing
Gui-Mei Tang: Conceptualization, Methodology, Project administration
Xiao-Min Chen: Data Curation
Yu-Song Wu: Investigation, Validation
Shi-Ning Wang: Visualization, Investigation

Declaration of Competing Interest

The authors declare that they have no known competing financial interests or personal relationships that could have appeared to influence the work reported in this paper.

Acknowledgments

This work was financially supported by Shandong Distinguished Middle-aged Young Scientist Encouragement and Reward Foundation (BS2011CL034), Shandong Provincial Natural Science Foundation (ZR2017MB041), and College Student Innovation and Entrepreneurship Training Program (S201910431065, S202010431073 and S202010431001).

Supplementary materials

Supplementary material associated with this article can be found, in the online version, at doi:[10.1016/j.molstruc.2021.130893](https://doi.org/10.1016/j.molstruc.2021.130893).

References

- [1] J.H. Askew, D.M. Pickup, G.O. Lloyd, A.V. Chadwick, H.J. Shepherd, Exploring the Effects of Synthetic and Postsynthetic Grinding on the Properties of the Spin Crossover Material Fe(atrz)(3) (BF4)(2) (atrz = 4-Amino-4H-1,2,4-Triazole), in: *Magnetochemistry*, 6, 2020, p. 44.
- [2] E.S. Bazhina, A.A. Bovkunova, A.V. Medved'ko, N.N. Efimov, M.A. Kiskin, I.L. Eremenko, Unusual Polynuclear Copper(II) Complexes with a Schiff-Base Ligand Containing Pyridyl and 1,2,4-Triazolyl Rings, *J. Cluster Sci.* 30 (2019) 1267–1275.
- [3] H. Begum, M.S. Ahmed, Y.-B. Kim, Nickel nanoflakes on 4-Amino-4H-1,2,4-Triazole/graphene for sustainable hydrogen evolution in acid and alkaline media, *Appl. Surf. Sci.* 515 (2020) 145999.
- [4] S.M. Gomha, M.M. Edrees, Z.A. Muhammad, N.A. Kheder, S. Abu-Melha, A.M. Saad, Synthesis, Characterization, and Antimicrobial Evaluation of Some New 1,4-Dihydropyridines-1,2,4-Triazole Hybrid Compounds, *Polycyclic Aromatic Compd.* (2020) 1–13.
- [5] S.M. Gomha, Z.A. Muhammad, E.E. El-Arab, A.M. Elmetwally, A.A. El-Sayed, I.K. Matar, Design, Synthesis, Molecular Docking Study and Anti-Hepatocellular Carcinoma Evaluation of New Bis-Triazolothiadiazines, *Mini-Rev. Med. Chem.* 20 (2020) 788–800.

- [6] D.A. Safin, K. Robeyns, Y. Garcia, 1,2,4-Triazole-based molecular switches: crystal structures, Hirshfeld surface analysis and optical properties, *CrystEngComm* 18 (2016) 7284–7296.
- [7] G. Yan, Q. Wu, Q. Hu, M. Li, Z. Zhang, W. Zhu, Theoretical design of novel high energy metal complexes based on two complementary oxygen-rich mixed ligands of 4-amino-4H-1,2,4-triazole-3,5-diol and 1,1'-dinitramino-5,5'-bistetraole, *J. Mol. Model.* 25 (2019) 340.
- [8] X.-X. Guo, D.-W. Gu, Z. Wu, W. Zhang, Copper-Catalyzed C–H Functionalization Reactions: efficient Synthesis of Heterocycles, *Chem. Rev.* 115 (2015) 1622–1651.
- [9] W.S. Bechara, I.S. Khazhieva, E. Rodriguez, A.B. Charette, One-Pot Synthesis of 3,4,5-Trisubstituted 1,2,4-Triazoles via the Addition of Hydrazides to Activated Secondary Amides, *Org. Lett.* 17 (2015) 1184–1187.
- [10] S. Maddila, R. Pagadala, S.B. Jonnalagadda, 1,2,4-Triazoles: a Review of Synthetic Approaches and the Biological Activity, *Lett. Org. Chem.* 10 (2013) 693–714.
- [11] H.Z. Zhang, G.L.V. Damu, G.X. Cai, C.H. Zhou, Current Developments in the Syntheses of 1, 2, 4-Triazole Compounds, *Curr. Org. Chem.* 18 (2014) 359–406.
- [12] M.L. Faschio, M.I. Errea, N.B. D'Accorso, Imidazothiazole and related heterocyclic systems. Synthesis, chemical and biological properties, *Eur. J. Med. Chem.* 90 (2015) 666–683.
- [13] R.S. Keri, S.A. Patil, S. Budagumpi, B.M. Nagaraja, Triazole: a Promising Antitubercular Agent, *Chem. Biol. Drug Des.* 86 (2015) 410–423.
- [14] I.A. Khan, M. Ahmad, S. Aslam, M.J. Saif, A.F. Zahoor, S.A.R. Naqvi, A. Mansha, Recent advances in the synthesis of triazole derivatives, *Afniadid* 72 (2015) 64–77.
- [15] S.G. Kucukguzel, P. Cikla-Suzgun, Recent advances bioactive 1, 2, 4-triazole-3-thiones, *Eur. J. Med. Chem.* 96 (2015) 830–870.
- [16] J.P. Zhang, Y.B. Zhang, J.B. Lin, X.M. Chen, Metal Azolate Frameworks: from Crystal Engineering to Functional Materials, *Chem. Rev.* 112 (2012) 1001–1033.
- [17] Y.-P. He, Y.-X. Tan, J. Zhang, Functional metal–organic frameworks constructed from triphenylamine-based polycarboxylate ligands, *Coord. Chem. Rev.* 420 (2020) 213354.
- [18] P. Wang, J.P. Ma, Y.B. Dong, R.Q. Huang, Tunable Luminescent Lanthanide Coordination Polymers Based on Reversible Solid-State Ion-Exchange Monitored by Ion-Dependent Photoinduced Emission Spectra, *J. Am. Chem. Soc.* 129 (2007) 10620–10621.
- [19] C.X. Xu, J.G. Zhang, X. Yin, X. Jin, T. Li, T.L. Zhang, Z.N. Zhou, Cd(II) complexes with different nuclearity and dimensionality based on 3-hydrazino-4-amino-1,2,4-triazole, *J. Solid State Chem.* 226 (2015) 59–65.
- [20] L.G. Lavrenova, O.G. Shakirova, Spin Crossover and Thermochromism of Iron(II) Coordination Compounds with 1,2,4-Triazoles and Tris(pyrazol-1-yl)methanes, *Eur. J. Inorg. Chem.* (2013) 670–682.
- [21] L. Kan, J. Cai, Z. Jin, G. Li, Y. Liu, L. Xu, Two Stable Zn-Cluster-Based Metal–Organic Frameworks with Breathing Behavior: synthesis, Structure, and Adsorption Properties, *Inorg. Chem.* 58 (2019) 391–396.
- [22] X.-N. Wang, P. Zhang, A. Kirchon, J.-L. Li, W.-M. Chen, Y.-M. Zhao, B. Li, H.-C. Zhou, Crystallographic Visualization of Postsynthetic Nickel Clusters into Metal–Organic Framework, *J. Am. Chem. Soc.* 141 (2019) 13654–13663.
- [23] R. Srivastava, L.R. Joshi, The effect of substituted 1,2,4-triazole moiety on the emission, phosphorescent properties of the blue emitting heteroleptic iridium(III) complexes and the OLED performance: a theoretical study, *Phys. Chem. Chem. Phys.* 16 (2014) 17284–17294.
- [24] D. Cakir, O. Bekircan, Z. Biyiklioglu, 1,2,4-Triazole-substituted metallophthalocyanines carrying redox active cobalt(II), manganese(III), titanium(IV) center and their electrochemical studies, *Synth. Met.* 201 (2015) 18–24.
- [25] H. Gao, J. n. M. Shreeve, Azole-Based Energetic Salts, *Chem. Rev.* 111 (2011) 7377–7436.
- [26] I.R. Ezabadi, C. Camoutsis, P. Zoumpoulakis, A. Geronikaki, M. Sokovic, J. Glamocilija, A. Ciric, Sulfonamide-1,2,4-triazole derivatives as antifungal and antibacterial agents: synthesis, biological evaluation, lipophilicity, and conformational studies, *Bioorg. Med. Chem.* 16 (2008) 1150–1161.
- [27] Y.A. Al-Soud, M.N. Al-Dwari, N.A. Al-Masoudi, Synthesis, antitumor and antiviral properties of some 1,2,4-triazole derivatives, *Farmaco* 59 (2004) 775–783.
- [28] A. Almasirad, S.A. Tabatabai, M. Faizi, A. Kebriaeezadeh, N. Mehrabi, A. Davvandi, A. Shafiee, Synthesis and anticonvulsant activity of new 2-substituted-5-[2-(2-fluorophenoxy)phenyl]-1,3,4-oxadiazoles and 1,2,4-triazoles, *Bioorg. Med. Chem. Lett.* 14 (2004) 6057–6059.
- [29] L. Shao, X. Zhou, Q. Zhang, J.B. Liu, Z. Jin, J.X. Fang, Synthesis, Structure, and Biological Activity of Novel 1H-1,2,4-Triazol-1-yl-thiazole Derivatives, *Synth. Commun.* 37 (2007) 199–207.
- [30] S.S. Kumar, H.P. Kavitha, Synthesis and Biological Applications of Triazole Derivatives - A Review, *Mini-Rev. Org. Chem.* 10 (2013) 40–65.
- [31] F. Bentiss, M. Lagrenée, D. Barbry, Accelerated synthesis of 3,5-disubstituted 4-amino-1,2,4-triazoles under microwave irradiation, *Tetrahedron Lett.* 41 (2000) 1539–1541.
- [32] S. Park, J. Jung, E.J. Cho, Visible-Light-Promoted Synthesis of Benzimidazoles, *Eur. J. Org. Chem.* 2014 (2014) 4148–4154.
- [33] Z.H. Xu, L.L. Han, G.L. Zhuang, J. Bai, D. Sun, In Situ Construction of Three Anion-Dependent Cu(I) Coordination Networks as Promising Heterogeneous Catalysts for Azide-Alkyne "Click" Reactions, *Inorg. Chem.* 54 (2015) 4737–4743.
- [34] L. Liu, Z.-B. Han, S.-M. Wang, D.-Q. Yuan, S.W. Ng, Robust Molecular Bowl-Based Metal–Organic Frameworks with Open Metal Sites: size Modulation To Increase the Catalytic Activity, *Inorg. Chem.* 54 (2015) 3719–3721.
- [35] L. Cheng, L.-M. Zhang, S.-H. Gou, Q.-N. Cao, J.-Q. Wang, L. Fang, Two temperature-controlled chiral Ag(I) coordination polymers with dual chiral components: synthesis, luminescence and SHG properties, *CrystEngComm* 14 (2012) 4437–4443.
- [36] J.-H. Wang, G.-M. Tang, Y.-T. Wang, T.-X. Qin, S.W. Ng, Metal-directed assembly of coordination polymers with the versatile ligand 2-(1H-benzotriazol-1-yl) acetic acid: from discrete structures to two-dimensional networks, *CrystEngComm* 16 (2014) 2660–2683.
- [37] J.-H. Wang, G.-M. Tang, Y.-T. Wang, Y.-Z. Cui, J.-J. Wang, S.W. Ng, A series of phenyl sulfonate metal coordination polymers as catalysts for one-pot Biginelli reactions under solvent-free conditions, *Dalton Trans.* 44 (2015) 17829–17840.
- [38] Y.T. Wang, G.M. Tang, Y.S. Wu, A Set of phenyl sulfonate metal coordination complexes triggered Biginelli reaction for the high efficient synthesis of 3,4-dihydropyrimidin-2(1H)-ones under solvent-free conditions, *Appl. Organomet. Chem.* 34 (2020) e5542.
- [39] Y.-T. Wang, G.-M. Tang, C.-C. Wang, Two d10 metal–organic frameworks based on a novel semi-rigid aromatic biscarboxylate ligand: syntheses, structures and luminescent properties, *Appl. Organomet. Chem.* 34 (2020) e5654.
- [40] E. Coronado, G. Minguez Espallargas, Dynamic magnetic MOFs, *Chem. Soc. Rev.* 42 (2013) 1525–1539.
- [41] A. Dhakshinamoorthy, H. Garcia, Metal–organic frameworks as solid catalysts for the synthesis of nitrogen-containing heterocycles, *Chem. Soc. Rev.* 43 (2014) 5750–5765.
- [42] J. Liu, L. Chen, H. Cui, J. Zhang, L. Zhang, C.Y. Su, Applications of metal–organic frameworks in heterogeneous supramolecular catalysis, *Chem. Soc. Rev.* 43 (2014) 6011–6061.
- [43] F. Sun, Z. Yin, Q.Q. Wang, D. Sun, M.H. Zeng, M. Kurmoo, Tandem Postsynthetic Modification of a MetalOrganic Framework by Thermal Elimination and Subsequent Bromination: effects on Absorption Properties and Photoluminescence, *Angew. Chem. Int. Ed.* 52 (2013) 4538–4543.
- [44] W.-X. Zhang, P.-Q. Liao, R.-B. Lin, Y.-S. Wei, M.-H. Zeng, X.-M. Chen, Metal cluster-based functional porous coordination polymers, *Coord. Chem. Rev.* 293–294 (2015) 263–278.
- [45] G.M. Sheldrick, SADABS, University of Göttingen, Göttingen, Germany, 1996 and 2003.
- [46] Bruker AXS, SAINT Software Reference Manual (1998).
- [47] G.M. Sheldrick, SHELXTL NT Version 5.1. Program for Solution and Refinement of Crystal Structures, University of Göttingen, Germany, 1997.
- [48] G.M. Sheldrick, A short history of SHELX, *Acta Crystallogr. Sect. A* 64 (2008) 112–122.
- [49] O.V. Dolomanov, L.J. Bourhis, R.J. Gildea, J.A.K. Howard, H. Puschmann, OLEX2: a complete structure solution, refinement and analysis program, *J. Appl. Cryst.* 42 (2009) 339–341.
- [50] A.L. Spek, Structure validation in chemical crystallography, *Acta Crystallogr., Sect. C-Biol. Crystallogr.* 65 (2009) 148–155.
- [51] M.J. Turner, J.J. McKinnon, S.K. Wolff, D.J. Grimwood, P.R. Spackman, D. Jayatilaka, M.A. Spackman, CrystalExplorer17, University of Western Australia, 2017 <http://hirschfeldsurface.net>.
- [52] J.H. Wang, G.M. Tang, Y.T. Wang, T.X. Qin, S.W. Ng, Metal-directed assembly of coordination polymers with the versatile ligand 2-(1H-benzotriazol-1-yl) acetic acid: from discrete structures to two-dimensional networks, *CrystEngComm* 16 (2014) 2660–2683.
- [53] Y.T. Wang, T.X. Qin, C. Zhao, G.M. Tang, T.D. Li, Y.Z. Cui, J.Y. Li, Two new one-dimensional luminescent silver(I) and lead(II) coordination polymers containing the flexible ligand 2-(1H-imidazole-1-yl)acetic acid, *J. Mol. Struct.* 938 (2009) 291–298.
- [54] S. Silong, M.Z. Ab Rahman, M. Hj Ahmad, H.C. Kwong, S.W. Ng, 3,5-Bis(4-hydroxy-phenyl)-4H-1,2,4-triazol-4-amine monohydrate, *Acta Crystallogr. Sect. E Struct. Rep. Online* 66 (2010) o2469–o2469.
- [55] M. Montazerohori, S. Mojahedi Jahromi, A. Masoudiasl, P. McArdle, Nano structure zinc (II) Schiff base complexes of a N3-tridentate ligand as new biological active agents: spectral, thermal behaviors and crystal structure of zinc azide complex, *Spectrochim. Acta A* 138 (2015) 517–528.
- [56] P. Wang, L. Zhao, Synthesis, structure and spectroscopic properties of the trinuclear cobalt(II) and nickel(II) complexes based on 2-hydroxynaphthaldehyde and bis(aminooxy)alkane, *Spectrochim. Acta, Part A* 135 (2015) 342–350.
- [57] C.-C. Wang, G.-M. Tang, Y.-T. Wang, J.-H. Wang, Y.-Z. Cui, S.-W. Ng, Syntheses, crystal structures, properties of metal coordination polymers based on a novel semi-rigid aromatic carboxylate ligand, *Polyhedron* 124 (2017) 145–155.
- [58] A.C. Tella, S.O. Owalude, A green route approach to the synthesis of Ni(II) and Zn(II) templated metal–organic frameworks, *J. Mater. Sci.* 49 (2014) 5635–5639.
- [59] J.M. Hao, Y.H. Li, H.H. Li, G.H. Cui, Two cobalt(II) metal–organic frameworks based on mixed 1,2,4,5-benzenetetracarboxylic acid and bis(benzimidazole) ligands, *Transition Met. Chem.* 39 (2013) 1–8.
- [60] M. Venkateshan, R.V. Priya, M. Muthu, J. Suresh, R.R. Kumar, Crystal structure, Hirshfeld surface analysis, DFT calculations and molecular docking studies on pyridine derivatives as potential inhibitors of NAMPT, *Chem. Data Coll.* 23 (2019) 100262.